Acta Cryst E CRYSTALLOGRAPHIC COMMUNICATIONS

ISSN 2056-9890

Photo-induced synthesis and structure of (benzo[4,5]imidazo[2,1-*b*]thiazol-2-yl)[4-(trifluoromethyl)phenyl]methanone

Yogesh Udayakumar,[a] Vignesh Balaraman,[b] Thisvanth Saravanakumar,[a] A. Aadithyan,[a] B. R. D. Yamajala Rajesh[b] and Sampath Natarajan[a]*

[a]Chemical Biology Lab, School of Chemical and Biotechnology, SASTRA Deemed University, Tirumalaisamudiram, Thanjavur-613401, Tamil Nadu, India, and [b]Organic Synthesis & Catalysis Lab, Department of Chemistry, School of Chemical and Biotechnology, SASTRA Deemed University, Thanjavur-613401, Tamil Nadu, India. *Correspondence e-mail: sampath@scbt.sastra.edu

Received 7 September 2026
Accepted 28 October 2026

Edited by T. Akitsu, Tokyo University of Science, Japan

Keywords: crystal structure; monoclinic; Hirshfeld Surface; dispersion forces; energy framework.

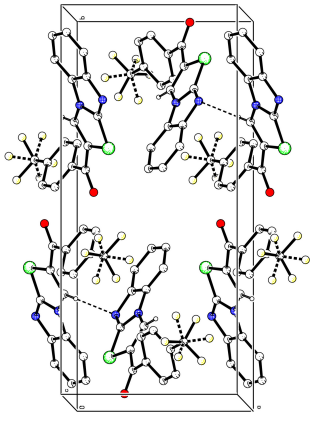
CCDC reference: 2598652

Supporting information: this article has supporting information at journals.iucr.org/e

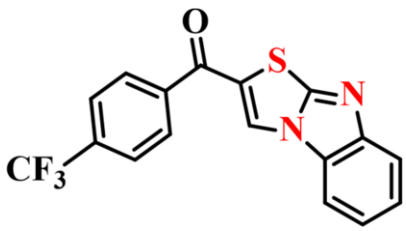
The title compound, $C_{17}H_9F_3N_2OS$, crystallizes in the monoclinic space group $P2_1/n$. The fused thiazolo[3,2-*a*]benzimidazole core is nearly planar, whereas the 4-(trifluoromethyl)phenyl ring is twisted by 52.6 (2)° from the thiazole ring. In the crystal, C—H···N hydrogen bonds form [101] chains, complemented by C—F···π and π–π contacts. Hirshfeld analysis reveals major H···F/F···H (21.4%) and C···H/H···C (17.5%) contributions. Energy-framework analysis shows that dispersion (−172.0 kJ mol^{-1}) dominates over Coulombic interactions (−53.8 kJ mol^{-1}), indicating that cumulative dispersion forces are primarily responsible for crystal cohesion.

1. Chemical context

Benzimidazole is a nitrogen-containing heterocyclic scaffold in medicinal chemistry, exhibiting a broad range of biological activities, including anticancer, antimicrobial, antiviral, anti-inflammatory and enzyme-inhibitory properties (Shrivastava *et al.*, 2017; Tahlan *et al.*, 2019*a*,*b*; Anichina *et al.*, 2017; Al-Rashood & Abdel-Aziz, 2010). Fusion of a thiazole ring with the benzimidazole framework affords thiazolo[3,2-*a*]benzimidazole derivatives with increased structural rigidity and extended π-conjugation, which can influence their pharmacological and physicochemical properties (Tahlan *et al.*, 2019*b*; Khaldi *et al.*, 2020; Ramos Rodríguez *et al.*, 2020). These fused heterocycles have also attracted interest as potential functional materials because of their tunable electronic and supramolecular characteristics. Their biological and physicochemical properties are closely related to molecular conformation, substituent effects and crystal-packing arrangements. Consequently, single-crystal X-ray diffraction is particularly valuable for establishing the molecular geometry and elucidating intermolecular interactions, including hydrogen bonding and aromatic stacking, that may contribute to structure–property relationships (Braga & Grepioni, 2000; Ramos Rodríguez *et al.*, 2020). Complementary Hirshfeld surface analysis and density functional theory calculations can provide further insight into the intermolecular contacts and electronic properties of these systems. As part of our ongoing investigations of fused and biologically relevant heterocycles (Al-Ansary *et al.*, 2017), we report here the synthesis and crystal structure of compound **3**, with particular emphasis on its molecular conformation and supramolecular assembly.



OPEN ACCESS
Published under a CC BY 4.0 licence



2. Structural commentary

The title compound **3**, $C_{17}H_9F_3N_2OS$ (Fig. 1), crystallizes in the centrosymmetric monoclinic space group $P2_1/n$. The molecular structure consists of a fused thiazolo[3,2-*a*]benzimidazole framework comprising benzene (*A*), imidazole (*B*) and thiazole (*C*) rings. The fused heterocyclic core is essentially planar, as indicated by the small interplanar angles of 0.72 (2), 0.57 (2) and 0.21 (3)°, respectively, between the *A*/*B*, *B*/*C* and *C*/*A* ring pairs. This pronounced coplanarity is consistent with related thiazolo[3,2-*a*]benzimidazole structures reported in the literature (Fun *et al.*, 2012*a*,*b*; Wang *et al.*, 2011). In contrast, the 4-(trifluoromethyl)phenyl ring (*D*), connected to the thiazole ring (*C*) is twisted appreciably, with a *C*/*D* dihedral angle of 52.6 (2)°. This deviation from coplanarity may result from a combination of steric interactions associated with the bulky –CF_3 substituent, electronic conjugation, and intermolecular interactions within the crystal. Similar variations in the orientation of aryl groups have been observed in related structures (Fun *et al.*, 2012*a*,*b*; Wang *et al.*, 2011), although the precise dihedral angle depends on the molecular connectivity and crystal-packing environment. The bond lengths and bond angles fall within the normal ranges for comparable heterocyclic compounds and agree well with standard crystallographic values (Allen *et al.*, 1987; Fun *et al.*, 2012*a*,*b*; Wang *et al.*, 2011). Overall, the structure exhibits a highly planar fused thiazolo[3,2-*a*]benzimidazole core, accompanied by a significantly twisted 4-(trifluoromethyl) phenyl ring.

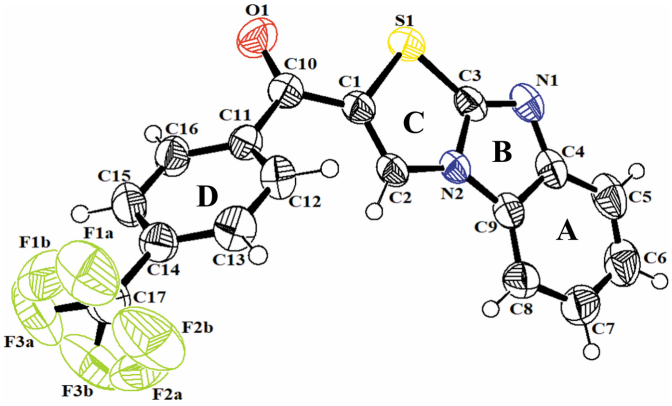


Figure 1
The molecular structure of the title compound, with displacement ellipsoids drawn at the 50% probability level.

Table 1
Hydrogen-bond geometry (Å, °).

D—H···*A*	*D*—H	H···*A*	*D*···*A*	*D*—H···*A*
C2—H2···N1^{i}	0.93	2.33	3.211 (2)	158
C13—H13···F2*B*	0.93	2.37	2.715 (10)	103
C15—H15···F3*A*	0.93	2.40	2.727 (6)	101

Symmetry code: (i) $x+\frac{1}{2}, -y+\frac{1}{2}, z+\frac{1}{2}$.

Table 2
C—F···*Cg* contacts (Å, °).

*Cg*1 and *Cg*2 are the centroids of the S1/C1/C2/N2/C3 and N1/C3/N2/C9/C4 rings, respectively.

C—F···*Cg*	C—F	F···*Cg*	C···*Cg*	C—F···*Cg*
C17—F1*A*···*Cg*1^{ii}	1.32 (1)	3.12 (1)	4.331 (3)	152 (1)
C17—F1*A*···*Cg*2^{ii}	1.32 (1)	3.51 (1)	4.309 (3)	119 (1)
C17—F2*B*···*Cg*1^{ii}	1.40 (1)	3.98 (1)	4.331 (3)	99 (1)
C17—F2*B*···*Cg*2^{ii}	1.40 (1)	3.29 (1)	4.309 (3)	129 (1)

Symmetry code: (ii) $x, y, z+1$.

The *para*-trifluoromethyl substituent in the title compound **3** exhibits rotational disorder, with the fluorine atoms distributed over two alternative orientations. Following refinement, the site-occupancy factors (SOFs) of the major and minor disorder components were refined to 0.701 (7) and 0.299 (7), respectively. This disorder is consistent with the presence of alternative orientations of the CF_3 group about the Csp^2—C(F_3) bond (C14—C17). Rotational disorder of CF_3 groups has been reported in related crystal structures, including (*E*)-4-(trifluoromethyl)benzaldehyde oxime (Jia *et al.*, 2006) and 3,5-bis(trifluoromethyl)pyrazolide anions (Phan *et al.*, 2010). The Hirshfeld surface reveals short contacts involving the fluorinated and aromatic regions of neighbouring molecules; however, these features alone do not confirm specific intermolecular interactions involving the disordered fluorine atoms. The overall crystal packing is supported by the intermolecular contacts established through crystallographic analysis.

Two weak intramolecular C—H···F contacts (Table 1) are present, which contribute to maintaining the molecular conformation.

3. Supramolecular features

The crystal packing of the title compound (**3**), viewed along the *a* axis, is illustrated in Fig. 2. The crystal structure is mainly governed by weak intermolecular C2—H2···N1 hydrogen bonds (Table 1), forming supramolecular chain propagating along the [101] direction. Furthermore, the crystal packing is reinforced by several C—F···π contacts (Table 2). Additionally, weak π–π contacts between the fused-ring system and the pendant phenyl ring are observed (Hunter & Sanders, 1990; Wang *et al.*, 2011), with centroid-to-centroid distances of *Cg*2···*Cg*4($-\frac{1}{2}+x, \frac{1}{2}-y, -\frac{1}{2}-z$) = 3.787 (1) Å and *Cg*3···*Cg*4($-\frac{1}{2}+x, \frac{1}{2}-y, -\frac{1}{2}-z$) = 3.772 (1) Å (*Cg*2, *Cg*3 and *Cg*4 are the centroids of the N1/C3/N2/C9/C4, C4–C9 and C11–C16 rings, respectively).

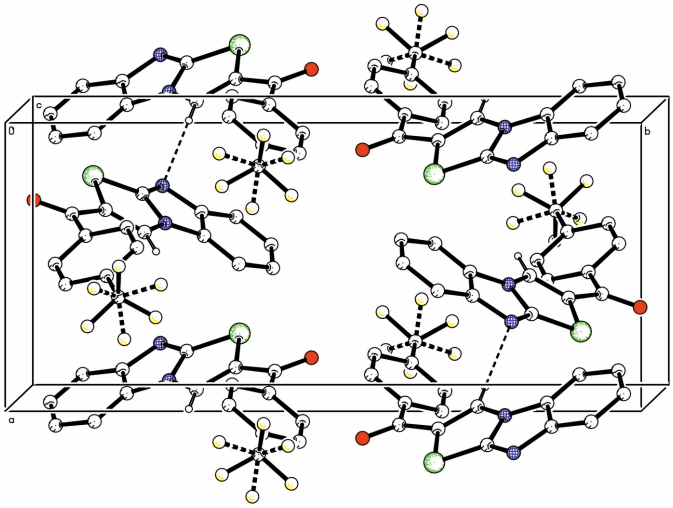


Figure 2
Crystal packing of compound (**3**) viewed along the *a* axis. Dashed lines indicate intermolecular C2—H2···N1 hydrogen bonds linking symmetry-related molecules into one-dimensional chains propagating along the [101] direction.

The Hirshfeld surface analysis provides quantitative support for the intermolecular interactions identified from the crystal structure. H···F/F···H contacts make the largest contribution (21.4%), highlighting the importance of fluorine-associated contacts and being consistent with the observed C—F···π interactions (Table 2). However, this contribution represents the overall close H···F contacts and cannot be attributed exclusively to C—F···π interactions. The N···H/H···N contacts contribute 9.3%, consistent with the inter-

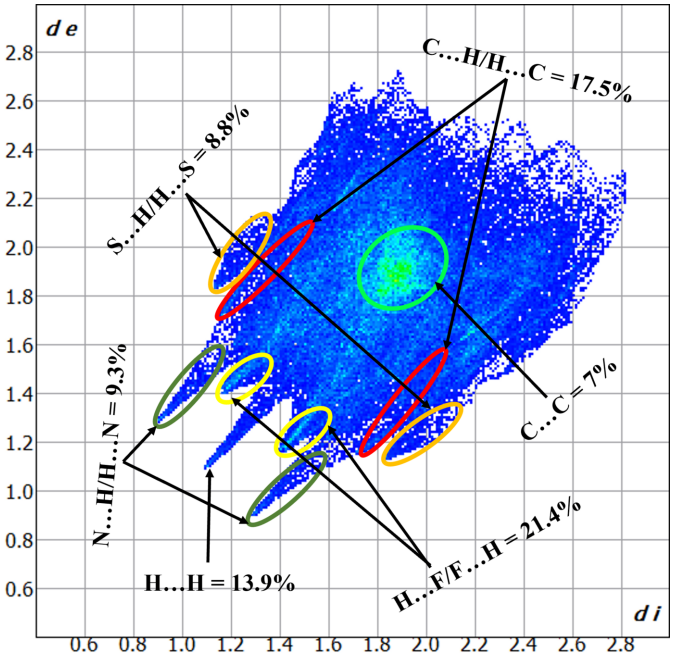


Figure 3
Two-dimensional fingerprint plots for compound (**3**), showing the percentage contributions of the major intermolecular contacts to the Hirshfeld surface.

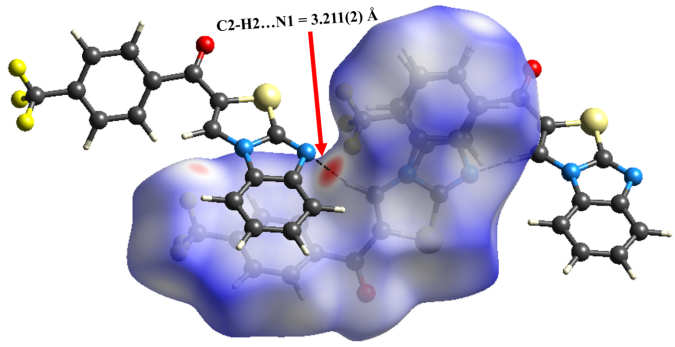


Figure 4
Hirshfeld surface (HS) of compound (**3**) mapped over d_{norm}, highlighting the principal intermolecular C—H···N contact contributing to crystal packing.

molecular C2—H2···N1 hydrogen bond, which generates the observed supramolecular chain. The C···C contacts (7.0%) are compatible with the aromatic contacts associated with the observed π–π interactions, although the fingerprint plot alone does not establish π-stacking. The substantial C···H/H···C (17.5%) and H···H (13.9%) contributions further indicate that dispersive and van der Waals contacts contribute significantly to the crystal architecture (Fig. 3). Overall, the crystallographic and Hirshfeld analyses are complementary: the former identifies specific C—H···N, C—F···π and π···π interactions, whereas the latter quantifies their broader intermolecular contact environment, showing that H···F/F···H, C···H/H···C, H···H and N···H/H···N contacts collectively dominate the packing.

The Hirshfeld surface (Spackman *et al.*, 2021) mapped over (d_{norm}) (Fig. 4) provides a visual depiction of the close intermolecular contacts in the crystal. The prominent red spots correspond to the C2—H2···N1 contact, confirming its directional nature and involvement in the supramolecular arrangement. Additional features observed on the Hirshfeld surface indicate short intermolecular contacts involving the fluorinated and aromatic regions of neighbouring molecules, consistent with the C—F···π and π–π interactions identified from the crystallographic analysis. However, these surface features provide supporting evidence rather than definitive confirmation of these specific interactions. Thus, the d_{norm} surface visually complements the crystallographic analysis by highlighting the principal regions of close molecular contact without implying that any single interaction alone governs the crystal cohesion.

The energy-framework analysis (Fig. 5) provides further insight into the energetic origin of the crystal packing. The pairwise intermolecular interaction energies were calculated for all molecular pairs within a 3.8 Å cluster of the reference molecule using *CrystalExplorer* (Spackman *et al.*, 2021). Summing these pairwise contributions gives a total interaction energy of −161.8 kJ mol^{-1} for the reference molecule, comprising a dispersion contribution of −172.0 kJ mol^{-1} and a Coulombic contribution of −53.8 kJ mol^{-1}. These values refer to the total interaction of the reference molecule with its first coordination sphere. They indicate that dispersion forces

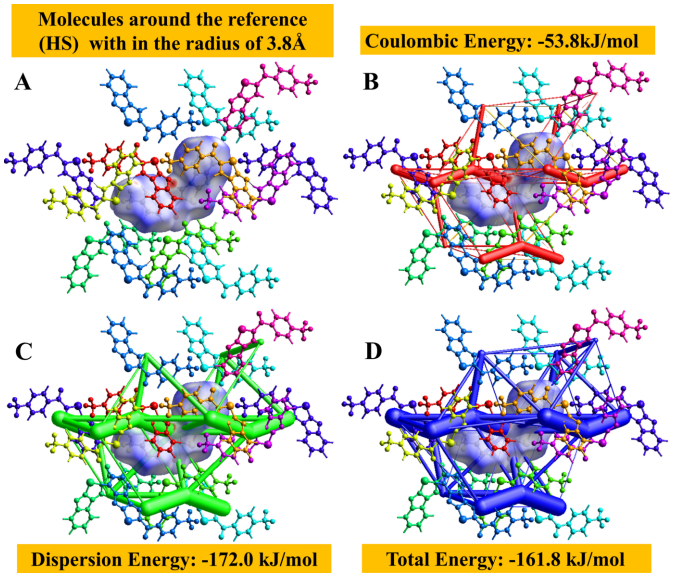


Figure 5
Energy-framework analysis of the crystal packing of compound (**3**): (A) Pairwise intermolecular interaction energies calculated for molecules within 3.8 Å of the reference molecule (HS); (B) Coulombic (E_{ele}); (C) dispersion (E_{dis}); and (D) total (E_{tot}) interaction energies, in kJ mol^{-1}. Negative values indicate consolidating interactions.

provide the dominant energetic contribution to the intermolecular consolidation within this cluster, although electrostatic interactions also contribute significantly. Therefore, the directional C—H···N hydrogen bonds, C—F···π contacts and π–π interactions help organize the molecules within the lattice, whereas the cumulative dispersion interactions provide the major energetic consolidation.

Overall, compound (**3**) exhibits stable crystal packing through a cooperative interplay of weak hydrogen bonding, C—F···π and π–π contacts and numerous close-contact interactions. Hirshfeld and d_{norm} analyses confirm the extensive intermolecular contact network, while the energy framework identifies dispersion (−172.0 kJ mol^{-1}) as the principal stabilizing force over the Coulombic contribution (−53.8 kJ mol^{-1}). Thus, directional interactions govern molecular organization, whereas cumulative dispersion forces provide the dominant energetic stabilization of the crystal packing.

4. Database survey

A systematic search of the Cambridge Structural Database (CSD, Version 5.47, November 2025 update; Groom *et al.*, 2016), conducted using the CCDC CONQUEST interface, identified two closely related thiazolobenzimidazole derivatives, namely benzo[4,5]imidazo[2,1-*b*]thiazol-2-yl(*p*-tolyl)-methanone and benzo[4,5]imidazo[2,1-*b*]thiazol-2-yl(4-fluorophenyl)methanone (CSD refcodes ABESUY and ABESOS; Ambethkar *et al.*, 2017). These derivatives contain *para*-methyl and *para*-fluoro substituents, respectively, on the benzoyl phenyl ring; however, despite their presence in the CSD, detailed crystallographic parameters are not readily available. A broader search for structurally related compounds containing the thiazolo[3,2-*a*]benzimidazole core identified additional entries, including BACCUH (Chen *et al.*, 2020) and AMUCIW (Yallur *et al.*, 2016). In these compounds, the benzoyl moiety is replaced by an aldehyde group, while their molecular geometries and conformational characteristics are closely comparable with those observed for the title compound **3**. The compounds CANHEI (Zhang *et al.*, 2021) and CANHEI01 (Chen *et al.*, 2022), which contain an unsubstituted benzoyl group, likewise display geometrical parameters that are in good agreement with those of compound **3**. The methyl ketone derivative FAQPAQ (Abdel-Aziz, Saleh & El-Zahabi, 2010), contains a closely related thiazolo[3,2-*a*]-benzimidazole moiety adopting an essentially planar conformation as observed in compound **3**. Other structurally related derivatives include the benzylidene-substituted compound EXIVOX (Wang *et al.*, 2011), in which no significant intermolecular hydrogen-bonding interactions were observed, and the analogous compound QECZAB (Fun *et al.*, 2012*b*), whose crystal packing is predominantly consolidated by π–π stacking interactions. Collectively, these crystallographic examples indicate that the thiazolo[3,2-*a*]benzimidazole core has a pronounced tendency to adopt an approximately planar conformation. In contrast, incorporation of a benzoyl substituent can result in rotation of the pendant phenyl ring with respect to the heteroaromatic core. The extent of this torsional deviation is influenced by the electronic and steric characteristics of the substituent, particularly when substitution occurs at the para position of the phenyl ring. The conformational features observed for the title compound are therefore consistent with the structural trends reported for related thiazolo[3,2-*a*]benzimidazole derivatives.

5. Synthesis and crystallization

The title compound **3** was synthesized (Fig. 6) by combining equal molar quantities of 2-mercaptobenzimidazole (**1**), enaminone (**2**), and *N*-methyl-2-pyrrolidone (NMP; 1 mL) in a borosilicate reaction tube equipped with an O_2-filled balloon. The reaction mixture was stirred under blue LED irradiation (2 × 14 W) for 4–6 h. The progress of the reaction was monitored by TLC. After completion, the reaction mixture was diluted with ethylacetate and washed with H_2O (2 × 15 mL). The organic layer was separated, dried over anhydrous Na_2SO_4, and concentrated under reduced pressure. The crude product was purified by column chromatography using hexane/ethylacetate (8:2, *v*/*v*) as the eluent. Colourless crystals

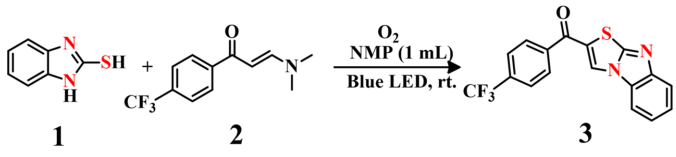


Figure 6
Synthesis of the title compound **3**.

suitable for single-crystal X-ray diffraction analysis were obtained by slow evaporation of an ethyl acetate solution at room temperature.

6. Refinement

Crystal data, data-collection parameters, and structure-refinement details are summarized in Table 3. Hydrogen atoms bonded to carbon were placed in geometrically calculated positions (C—H = 0.93 Å) and refined using a riding model, with their isotropic displacement parameters fixed at U_{iso}(H) = 1.2Ueq(C). The CF_3 group is disordered over two orientations. The site-occupancy factors refined to 0.701 (7) and 0.299 (7). Two fluorine atoms in each component showed elongated displacement ellipsoids and were each modelled as split over two positions. SADI, SIMU and RIGU restraints were applied to the disordered group (114 restraints in total). Final $R1$ = 0.043 for $I > 2\sigma(I)$ and $wR2$ = 0.107 for all data.

Table 3
Experimental details.

Crystal data	
Chemical formula	$C_{17}H_9F_3N_2OS$
M_r	346.32
Crystal system, space group	Monoclinic, $P2_1/n$
Temperature (K)	293
a, b, c (Å)	8.5887 (9), 18.995 (2), 9.4591 (9)
β (°)	94.774 (3)
V (Å^3)	1537.8 (3)
Z	4
Radiation type	Mo $K\alpha$
μ (mm^{-1})	0.25
Crystal size (mm)	0.28 × 0.16 × 0.12
Data collection	
Diffractometer	Bruker APEXII CCD
No. of measured, independent and observed [$I > 2\sigma(I)$] reflections	37328, 3827, 2632
R_{int}	0.050
(sin $\theta/\lambda)_{max}$ (Å^{-1})	0.667
Refinement	
$R[F^2 > 2\sigma(F^2)]$, $wR(F^2)$, S	0.043, 0.107, 1.03
No. of reflections	3827
No. of parameters	246
No. of restraints	114
H-atom treatment	H-atom parameters constrained
$\Delta\rho_{max}$, $\Delta\rho_{min}$ (e Å^{-3})	0.21, −0.29

Computer programs: *APEX3* and *SAINT* (Bruker, 2017), *SHELXT2018/2* (Sheldrick, 2015*a*), *SHELXL2025/1* (Sheldrick, 2015*b*) and *OLEX2* (Dolomanov *et al.*, 2009).

Acknowledgements

The authors gratefully acknowledge the Vellore Institute of Technology (VIT) for providing the single crystal X-ray diffraction data.

References

Abdel–Aziz, H. A., Saleh, T. S. & El–Zahabi, H. S. A. (2010). *Arch. Pharm.* **343**, 24–30.
Al-Ansary, G. H., Eldehna, W. M., Ghabbour, H. A., Al-Rashood, S. T., Al-Rashood, K. A., Eladwy, R. A., Al-Dhfyan, A., Kabil, M. M. & Abdel-Aziz, H. A. (2017). *J. Enzyme Inhib. Med. Chem.* **32**, 986–991.
Allen, F. H., Kennard, O., Watson, D. G., Brammer, L., Orpen, A. G. & Taylor, R. (1987). *J. Chem. Soc. Perkin Trans. 2* pp. S1–S19.
Al-Rashood, S. T. & Abdel-Aziz, H. A. (2010). *Molecules* **15**, 3775–3815.
Ambethkar, S., Vellimalai, M., Padmini, V. & Bhuvanesh, N. (2017). *New J. Chem.* **41**, 75–80.
Anichina, K., Mavrova, A., Yancheva, D., Tsenov, J. & Dimitrov, R. (2017). *J. Mol. Struct.* **1150**, 179–187.
Braga, D. & Grepioni, F. (2000). *Acc. Chem. Res.* **33**, 601–608.
Bruker (2017). *APEX3* and *SAINT*. Bruker AXS Inc., Madison, Wisconsin, USA.
Chen, Z., Jin, W., Xia, Y., Zhang, Y., Xie, M., Ma, S. & Liu, C. (2020). *Org. Lett.* **22**, 8261–8266.
Chen, Z., Xue, F., Zhang, Y., Jin, W., Wang, B., Xia, Y., Xie, M., Abdukader, A. & Liu, C. (2022). *Org. Lett.* **24**, 3149–3154.
Dolomanov, O. V., Bourhis, L. J., Gildea, R. J., Howard, J. A. K. & Puschmann, H. (2009). *J. Appl. Cryst.* **42**, 339–341.
Fun, H.-K., Chantrapromma, S. & Abdel-Aziz, H. A. (2012*a*). *Acta Cryst.* E**68**, o1393–o1394.
Fun, H.-K., Quah, C. K., Abdel-Aziz, H. A. & Ghabbour, H. A. (2012*b*). *Acta Cryst.* E**68**, o2705.
Groom, C. R., Bruno, I. J., Lightfoot, M. P. & Ward, S. C. (2016). *Acta Cryst.* B**72**, 171–179.
Hunter, C. A. & Sanders, J. K. M. (1990). *J. Am. Chem. Soc.* **112**, 5525–5534.
Jia, J., Wang, X.-Z., Zhang, Y. & Wang, J.-W. (2006). *Acta Cryst.* E**62**, o2683–o2684.
Khaldi, H., Djafri, A., Megrouss, Y., Khelloul, N., Chouaih, A. & Djafri, A. (2020). *Acta Cryst.* E**76**, 1832–1836.
Phan, H. N., Lerner, H.-W. & Bolte, M. (2010). *Acta Cryst.* E**66**, m928.
Ramos Rodríguez, O. A., Magaña Vergara, N. E., Mojica Sánchez, J. P., Sumaya Martínez, M. T., Gómez Sandoval, Z., Cruz, A. & Ramos Organillo, Á. (2020). *J. Mol. Struct.* **1199**, 127036.
Sheldrick, G. M. (2015*a*). *Acta Cryst.* A**71**, 3–8.
Sheldrick, G. M. (2015*b*). *Acta Cryst.* C**71**, 3–8.
Shrivastava, N., Naim, M. J., Alam, M. J., Nawaz, F., Ahmed, S. & Alam, O. (2017). *Arch. Pharm.* **350**, e201700040.
Spackman, P. R., Turner, M. J., McKinnon, J. J., Wolff, S. K., Grimwood, D. J., Jayatilaka, D. & Spackman, M. A. (2021). *J. Appl. Cryst.* **54**, 1006–1011.
Tahlan, S., Kumar, S. & Narasimhan, B. (2019*a*). *BMC Chem.* **13**, 18.
Tahlan, S., Kumar, S. & Narasimhan, B. (2019*b*). *BMC Chem.* **13**, 101.
Wang, Z.-M., Yu, B., Cui, Y., Zhang, X.-Q. & Sun, X.-Q. (2011). *Acta Cryst.* E**67**, o2540.
Yallur, B., Krishna, P. M. & Hosamani, A. A. (2016). *IUCrData* **1**, x160778.
Zhang, J., She, M., Liu, L., Feng, X., Li, Y., Liu, H., Zheng, T., Leng, X., Liu, P., Zhang, S. & Li, J. (2021). *Org. Lett.* **23**, 8396–8401.

supporting information

Acta Cryst. (2026). E**82** [https://doi.org/10.1107/S2056989026011230]

Photo-induced synthesis and structure of (benzo[4,5]imidazo[2,1-*b*]thiazol-2-yl)[4-(trifluoromethyl)phenyl]methanone

Yogesh Udayakumar, Vignesh Balaraman, Thisvanth Saravanakumar, A. Aadithyan, B. R. D. Yamajala Rajesh and Sampath Natarajan

Computing details

(Benzo[4,5]imidazo[2,1-*b*]thiazol-2-yl)[4-(trifluoromethyl)phenyl]methanone

Crystal data

$C_{17}H_9F_3N_2OS$
M_r = 346.32
Monoclinic, $P2_1/n$
a = 8.5887 (9) Å
b = 18.995 (2) Å
c = 9.4591 (9) Å
β = 94.774 (3)°
V = 1537.8 (3) Å^3
Z = 4
$F(000)$ = 704
D_x = 1.496 Mg m^{-3}
Mo $K\alpha$ radiation, λ = 0.71073 Å
Cell parameters from 37328 reflections
θ = 2.1–28.3°
μ = 0.25 mm^{-1}
T = 293 K
Block, colourless
0.28 × 0.16 × 0.12 mm

Data collection

Bruker APEXII CCD diffractometer
φ and ω scans
37328 measured reflections
3827 independent reflections
2632 reflections with $I > 2\sigma(I)$
R_{int} = 0.050
θ_{max} = 28.3°, θ_{min} = 2.1°
h = −11→11
k = −25→25
l = −12→12

Refinement

Refinement on F^2
Least-squares matrix: full
$R[F^2 > 2\sigma(F^2)]$ = 0.043
$wR(F^2)$ = 0.107
S = 1.03
3827 reflections
246 parameters
114 restraints
Hydrogen site location: inferred from neighbouring sites
H-atom parameters constrained
$w = 1/[\sigma^2(F_o^2) + (0.029P)^2 + 0.786P]$ where $P = (F_o^2 + 2F_c^2)/3$
$(\Delta/\sigma)_{max} < 0.001$
$\Delta\rho_{max}$ = 0.21 e Å^{-3}
$\Delta\rho_{min}$ = −0.29 e Å^{-3}
Extinction correction: SHELXL-2025/1 (Sheldrick 2015a), $Fc^*=kFc[1+0.001xFc^2\lambda^3/\sin(2\theta)]^{-1/4}$
Extinction coefficient: 0.0035 (7)

Special details

Geometry. All esds (except the esd in the dihedral angle between two l.s. planes) are estimated using the full covariance matrix. The cell esds are taken into account individually in the estimation of esds in distances, angles and torsion angles; correlations between esds in cell parameters are only used when they are defined by crystal symmetry. An approximate (isotropic) treatment of cell esds is used for estimating esds involving l.s. planes.

Fractional atomic coordinates and isotropic or equivalent isotropic displacement parameters (Å²)

	x	*y*	*z*	U_{iso}*/U_{eq}	Occ. (<1)
S1	0.21482 (6)	0.12390 (3)	0.33024 (5)	0.05476 (17)	
F1A	0.6110 (4)	0.1253 (3)	1.2294 (3)	0.0955 (13)	0.701 (7)
F1B	0.6865 (17)	0.0865 (6)	1.2212 (9)	0.147 (6)	0.299 (7)
F2A	0.7790 (7)	0.1870 (2)	1.1381 (4)	0.128 (2)	0.701 (7)
F2B	0.6701 (12)	0.1933 (5)	1.1883 (10)	0.117 (4)	0.299 (7)
F3A	0.8126 (5)	0.0787 (2)	1.1641 (4)	0.1149 (17)	0.701 (7)
F3B	0.8535 (7)	0.1385 (7)	1.1237 (7)	0.104 (4)	0.299 (7)
O1	0.31967 (19)	0.02097 (7)	0.55604 (16)	0.0671 (4)	
N1	0.23203 (19)	0.24075 (9)	0.14990 (16)	0.0533 (4)	
N2	0.38054 (16)	0.23609 (8)	0.35833 (15)	0.0411 (3)	
C1	0.3455 (2)	0.13667 (9)	0.48196 (18)	0.0428 (4)	
C2	0.4228 (2)	0.19826 (9)	0.47840 (18)	0.0418 (4)	
H2	0.496548	0.213344	0.549530	0.050*	
C3	0.2698 (2)	0.20429 (10)	0.26496 (19)	0.0457 (4)	
C4	0.3249 (2)	0.30140 (11)	0.1681 (2)	0.0500 (5)	
C5	0.3333 (3)	0.35976 (13)	0.0801 (2)	0.0681 (7)	
H5	0.272716	0.362671	−0.005837	0.082*	
C6	0.4340 (3)	0.41276 (14)	0.1245 (3)	0.0762 (7)	
H6	0.440577	0.452223	0.067152	0.091*	
C7	0.5263 (3)	0.40982 (13)	0.2518 (3)	0.0702 (7)	
H7	0.593182	0.447031	0.277306	0.084*	
C8	0.5207 (2)	0.35272 (11)	0.3411 (2)	0.0569 (5)	
H8	0.582374	0.350123	0.426513	0.068*	
C9	0.4187 (2)	0.29975 (10)	0.29673 (19)	0.0444 (4)	
C10	0.3690 (2)	0.07979 (10)	0.5852 (2)	0.0463 (4)	
C11	0.4576 (2)	0.09501 (9)	0.72468 (18)	0.0419 (4)	
C12	0.4361 (2)	0.15625 (10)	0.8002 (2)	0.0496 (5)	
H12	0.366730	0.190400	0.762928	0.059*	
C13	0.5175 (2)	0.16671 (11)	0.9309 (2)	0.0533 (5)	
H13	0.502156	0.207715	0.981689	0.064*	
C14	0.6211 (2)	0.11662 (10)	0.98605 (19)	0.0484 (5)	
C15	0.6431 (2)	0.05546 (11)	0.9116 (2)	0.0574 (5)	
H15	0.713178	0.021617	0.948954	0.069*	
C16	0.5612 (2)	0.04457 (10)	0.7821 (2)	0.0517 (5)	
H16	0.575506	0.003058	0.732714	0.062*	
C17	0.7076 (3)	0.12874 (12)	1.1281 (2)	0.0630 (6)	

Atomic displacement parameters (Å²)

	U^{11}	U^{22}	U^{33}	U^{12}	U^{13}	U^{23}
S1	0.0536 (3)	0.0547 (3)	0.0526 (3)	−0.0066 (2)	−0.0162 (2)	−0.0027 (2)
F1A	0.099 (2)	0.149 (4)	0.0384 (13)	−0.001 (2)	0.0056 (12)	−0.0022 (17)
F1B	0.211 (12)	0.140 (8)	0.076 (6)	−0.112 (8)	−0.065 (7)	0.073 (6)
F2A	0.195 (6)	0.102 (3)	0.078 (2)	−0.092 (3)	−0.049 (3)	0.025 (2)
F2B	0.114 (6)	0.131 (6)	0.098 (6)	0.028 (5)	−0.034 (5)	−0.064 (5)
F3A	0.122 (3)	0.124 (3)	0.089 (2)	0.045 (2)	−0.053 (2)	−0.010 (2)
F3B	0.065 (3)	0.183 (11)	0.062 (3)	−0.004 (5)	−0.018 (3)	−0.008 (6)
O1	0.0851 (11)	0.0477 (8)	0.0654 (9)	−0.0147 (8)	−0.0118 (8)	0.0012 (7)
N1	0.0491 (9)	0.0680 (11)	0.0408 (9)	0.0088 (8)	−0.0086 (7)	0.0038 (8)
N2	0.0389 (8)	0.0453 (8)	0.0376 (8)	0.0022 (6)	−0.0056 (6)	0.0024 (6)
C1	0.0417 (10)	0.0455 (10)	0.0398 (9)	−0.0005 (8)	−0.0051 (7)	−0.0012 (8)
C2	0.0393 (9)	0.0478 (10)	0.0366 (9)	0.0015 (8)	−0.0074 (7)	0.0014 (8)
C3	0.0396 (10)	0.0548 (11)	0.0407 (9)	0.0065 (8)	−0.0083 (8)	−0.0044 (8)
C4	0.0428 (10)	0.0639 (12)	0.0434 (10)	0.0131 (9)	0.0035 (8)	0.0111 (9)
C5	0.0566 (13)	0.0901 (17)	0.0578 (13)	0.0160 (12)	0.0058 (11)	0.0291 (12)
C6	0.0614 (15)	0.0788 (17)	0.0909 (18)	0.0098 (13)	0.0205 (13)	0.0423 (14)
C7	0.0558 (13)	0.0633 (14)	0.0924 (18)	−0.0047 (11)	0.0112 (13)	0.0211 (13)
C8	0.0486 (11)	0.0577 (12)	0.0639 (13)	−0.0028 (9)	0.0021 (10)	0.0098 (10)
C9	0.0391 (10)	0.0503 (10)	0.0438 (10)	0.0067 (8)	0.0035 (8)	0.0075 (8)
C10	0.0464 (10)	0.0456 (10)	0.0463 (10)	−0.0010 (8)	0.0009 (8)	0.0003 (8)
C11	0.0433 (10)	0.0421 (9)	0.0403 (9)	−0.0023 (8)	0.0037 (8)	0.0051 (8)
C12	0.0534 (11)	0.0492 (11)	0.0457 (11)	0.0100 (9)	0.0020 (9)	0.0028 (8)
C13	0.0655 (13)	0.0519 (11)	0.0432 (11)	0.0031 (10)	0.0079 (9)	−0.0051 (9)
C14	0.0501 (11)	0.0559 (11)	0.0389 (10)	−0.0053 (9)	0.0026 (8)	0.0070 (9)
C15	0.0605 (13)	0.0542 (12)	0.0555 (12)	0.0087 (10)	−0.0069 (10)	0.0089 (10)
C16	0.0606 (12)	0.0420 (10)	0.0516 (11)	0.0049 (9)	−0.0017 (9)	0.0009 (9)
C17	0.0748 (16)	0.0705 (15)	0.0426 (11)	−0.0094 (12)	−0.0015 (11)	0.0072 (11)

Geometric parameters (Å, º)

S1—C1	1.7635 (17)	C5—C6	1.370 (3)
S1—C3	1.728 (2)	C6—H6	0.9300
F1A—C17	1.320 (3)	C6—C7	1.386 (3)
F1B—C17	1.216 (6)	C7—H7	0.9300
F2A—C17	1.264 (3)	C7—C8	1.378 (3)
F2B—C17	1.400 (6)	C8—H8	0.9300
F3A—C17	1.335 (3)	C8—C9	1.377 (3)
F3B—C17	1.271 (6)	C10—C11	1.496 (2)
O1—C10	1.218 (2)	C11—C12	1.386 (3)
N1—C3	1.308 (2)	C11—C16	1.387 (3)
N1—C4	1.404 (3)	C12—H12	0.9300
N2—C2	1.367 (2)	C12—C13	1.383 (3)
N2—C3	1.382 (2)	C13—H13	0.9300
N2—C9	1.393 (2)	C13—C14	1.375 (3)
C1—C2	1.347 (2)	C14—C15	1.379 (3)

C1—C10	1.459 (2)	C14—C17	1.498 (3)
C2—H2	0.9300	C15—H15	0.9300
C4—C5	1.392 (3)	C15—C16	1.376 (3)
C4—C9	1.402 (2)	C16—H16	0.9300
C5—H5	0.9300		

C3—S1—C1	89.70 (8)	O1—C10—C11	121.25 (17)
C3—N1—C4	103.48 (15)	C1—C10—C11	118.63 (16)
C2—N2—C3	114.97 (15)	C12—C11—C10	122.48 (16)
C2—N2—C9	138.44 (15)	C12—C11—C16	119.13 (17)
C3—N2—C9	106.58 (14)	C16—C11—C10	118.36 (17)
C2—C1—S1	112.39 (13)	C11—C12—H12	119.9
C2—C1—C10	128.24 (16)	C13—C12—C11	120.14 (18)
C10—C1—S1	119.07 (13)	C13—C12—H12	119.9
N2—C2—H2	123.8	C12—C13—H13	119.9
C1—C2—N2	112.33 (15)	C14—C13—C12	120.15 (18)
C1—C2—H2	123.8	C14—C13—H13	119.9
N1—C3—S1	135.16 (15)	C13—C14—C15	120.08 (18)
N1—C3—N2	114.22 (17)	C13—C14—C17	119.38 (19)
N2—C3—S1	110.62 (13)	C15—C14—C17	120.54 (19)
C5—C4—N1	129.59 (19)	C14—C15—H15	120.0
C5—C4—C9	118.8 (2)	C16—C15—C14	119.94 (19)
C9—C4—N1	111.57 (16)	C16—C15—H15	120.0
C4—C5—H5	121.2	C11—C16—H16	119.7
C6—C5—C4	117.7 (2)	C15—C16—C11	120.55 (18)
C6—C5—H5	121.2	C15—C16—H16	119.7
C5—C6—H6	118.7	F1A—C17—F3A	103.4 (3)
C5—C6—C7	122.5 (2)	F1A—C17—C14	110.4 (2)
C7—C6—H6	118.7	F1B—C17—F2B	103.2 (6)
C6—C7—H7	119.4	F1B—C17—F3B	109.1 (6)
C8—C7—C6	121.2 (2)	F1B—C17—C14	117.1 (4)
C8—C7—H7	119.4	F2A—C17—F1A	108.6 (3)
C7—C8—H8	121.9	F2A—C17—F3A	106.9 (3)
C9—C8—C7	116.2 (2)	F2A—C17—C14	113.7 (2)
C9—C8—H8	121.9	F2B—C17—C14	112.7 (4)
N2—C9—C4	104.15 (16)	F3A—C17—C14	113.2 (2)
C8—C9—N2	132.28 (17)	F3B—C17—F2B	98.4 (5)
C8—C9—C4	123.57 (18)	F3B—C17—C14	114.2 (3)
O1—C10—C1	120.10 (17)		

S1—C1—C2—N2	0.3 (2)	C6—C7—C8—C9	−0.2 (3)
S1—C1—C10—O1	11.9 (3)	C7—C8—C9—N2	−178.9 (2)
S1—C1—C10—C11	−169.56 (13)	C7—C8—C9—C4	0.7 (3)
O1—C10—C11—C12	−139.6 (2)	C9—N2—C2—C1	−179.05 (19)
O1—C10—C11—C16	38.2 (3)	C9—N2—C3—S1	179.45 (12)
N1—C4—C5—C6	179.3 (2)	C9—N2—C3—N1	−0.2 (2)
N1—C4—C9—N2	−0.2 (2)	C9—C4—C5—C6	0.1 (3)
N1—C4—C9—C8	−179.90 (18)	C10—C1—C2—N2	173.84 (17)

C1—S1—C3—N1	179.4 (2)	C10—C11—C12—C13	177.92 (18)
C1—S1—C3—N2	−0.22 (14)	C10—C11—C16—C15	−178.62 (18)
C1—C10—C11—C12	41.9 (3)	C11—C12—C13—C14	0.5 (3)
C1—C10—C11—C16	−140.32 (18)	C12—C11—C16—C15	−0.8 (3)
C2—N2—C3—S1	0.45 (19)	C12—C13—C14—C15	−0.6 (3)
C2—N2—C3—N1	−179.23 (16)	C12—C13—C14—C17	−179.72 (19)
C2—N2—C9—C4	178.9 (2)	C13—C14—C15—C16	0.0 (3)
C2—N2—C9—C8	−1.5 (4)	C13—C14—C17—F1A	69.4 (3)
C2—C1—C10—O1	−161.2 (2)	C13—C14—C17—F1B	119.0 (10)
C2—C1—C10—C11	17.3 (3)	C13—C14—C17—F2A	−53.0 (5)
C3—S1—C1—C2	−0.06 (15)	C13—C14—C17—F2B	−0.5 (7)
C3—S1—C1—C10	−174.23 (16)	C13—C14—C17—F3A	−175.2 (3)
C3—N1—C4—C5	−179.1 (2)	C13—C14—C17—F3B	−111.7 (7)
C3—N1—C4—C9	0.1 (2)	C14—C15—C16—C11	0.7 (3)
C3—N2—C2—C1	−0.5 (2)	C15—C14—C17—F1A	−109.8 (3)
C3—N2—C9—C4	0.26 (19)	C15—C14—C17—F1B	−60.1 (11)
C3—N2—C9—C8	179.9 (2)	C15—C14—C17—F2A	127.8 (4)
C4—N1—C3—S1	−179.49 (17)	C15—C14—C17—F2B	−179.6 (7)
C4—N1—C3—N2	0.1 (2)	C15—C14—C17—F3A	5.6 (4)
C4—C5—C6—C7	0.3 (4)	C15—C14—C17—F3B	69.1 (7)
C5—C4—C9—N2	179.06 (17)	C16—C11—C12—C13	0.2 (3)
C5—C4—C9—C8	−0.6 (3)	C17—C14—C15—C16	179.11 (19)
C5—C6—C7—C8	−0.2 (4)		

Hydrogen-bond geometry (Å, º)

*Cg*1 and *Cg*2 are the centroids of the S1/C1/C2/N2/C3 and N1/C3/N2/C9/C4 rings, respectively.

D—H···*A*	*D*—H	H···*A*	*D*···*A*	*D*—H···*A*
C2—H2···N1^{i}	0.93	2.33	3.211 (2)	158
C13—H13···F2*B*	0.93	2.37	2.715 (10)	103
C15—H15···F3*A*	0.93	2.40	2.727 (6)	101
C17—F1*A*···Cg1^{ii}	1.32 (1)	3.12 (1)	4.331 (3)	152 (1)
C17—F1*A*···Cg2^{ii}	1.32 (1)	3.51 (1)	4.309 (3)	119 (1)
C17—F2*B*···Cg1^{ii}	1.40 (1)	3.98 (1)	4.331 (3)	99 (1)
C17—F2*B*···Cg2^{ii}	1.40 (1)	3.29 (1)	4.309 (3)	129 (1)

Symmetry codes: (i) *x*+1/2, −*y*+1/2, *z*+1/2; (ii) *x*, *y*, *z*+1.